

High-Resolution ^{39}K NMR Spectroscopy of Bio-organic Solids

Gang Wu,^{*,†} Zhehong Gan,[‡] Irene C. M. Kwan,[†] James C. Fetters,^{§,||} and Jeffery T. Davis[§]

[†]Department of Chemistry, Queen's University, Kingston, Ontario, Canada K7L 3N6

[‡]Center of Interdisciplinary Magnetic Resonance, National High Magnetic Field Laboratory, 1800 East Paul Dirac Drive, Tallahassee, Florida 32310, United States

[§]Department of Chemistry and Biochemistry, University of Maryland, College Park, Maryland 20742, United States

S Supporting Information

ABSTRACT: We report the first implementation of the multiple-quantum magic-angle-spinning method to obtain high-resolution ^{39}K NMR spectra for bio-organic solids. The observed spectral resolution in the isotropic dimension is nearly at the sub-ppm level, which approaches the intrinsic resolution limit determined primarily by quadrupole relaxation. We show that high-resolution solid-state ^{39}K NMR spectroscopy can be used as a new means of probing K^+ ions in biomolecular systems.

The importance of K^+ ions in biological structures and processes has been well-documented in the literature.^{1–3} As a member of group IA, K^+ ions are invisible to spectroscopic detection methods such as UV–vis and electron paramagnetic resonance (EPR). Although one of the stable K isotopes, ^{39}K ($I = 3/2$, natural abundance 93%), can be studied by NMR spectroscopy, the actual NMR receptivity of ^{39}K is exceedingly low. In fact, ^{39}K is among the so-called low- γ quadrupolar nuclides, which are notoriously difficult to study by solid-state NMR spectroscopy.^{4–6} As a result, crystallography is to date the only biophysical technique that can provide detailed information about the localization and chemical environment of K^+ ions in biomolecular structures. Notable examples include crystallographic studies of K^+ -activated enzymes,^{7–9} ion channel proteins,^{10–12} DNA G-quadruplexes,^{13,14} and group-I intron ribozymes.¹⁵ In recent years, magic-angle-spinning (MAS) ^{39}K NMR spectroscopy at very high magnetic fields has shown promising signs of becoming a valid analytical method for detecting K^+ ions in inorganic, organic, and biological solids.^{16–24} However, one major obstacle in ^{39}K MAS NMR applications is that the achievable spectral resolution is rather limited. Two factors are in play in this regard. One is that the MAS technique itself can only partially remove the second-order quadrupole line broadening. The other is that the combination of a relatively small ^{39}K chemical shift range (ca. 100 ppm) and a very low ^{39}K Larmor frequency (4.7% of the ^1H Larmor frequency) usually makes the chemical shift dispersion between different ^{39}K NMR signals considerably smaller than the residual second-order quadrupolar broadening of the individual signals. Consequently, ^{39}K NMR signals from K^+ ions in different chemical environments are often severely overlapped in the MAS NMR spectrum, making it particularly difficult to extract useful chemical information. Although advanced NMR methods such as double rotation (DOR),^{25–27} dynamic-angle spinning (DAS),^{28,29} multiple-quantum MAS (MQMAS),^{30,31} and satellite-transition MAS (STMAS)³² can in

principle be used to produce high-resolution NMR spectra, for all half-integer quadrupolar nuclei (including ^{39}K), these techniques have not been successfully implemented in ^{39}K NMR spectroscopy to date, except for one STMAS ^{39}K NMR spectrum of K_2SO_4 (molecular weight = 174 Da) reported by Wimperis and co-workers.³³ Clearly, the primary difficulty stems from the low ^{39}K NMR receptivity. Here we report the first utilization of the MQMAS method to obtain high-resolution ^{39}K NMR spectra for bio-organic solids. The strategy employed in the present study to overcome the practical difficulties in detecting very weak ^{39}K MQMAS signals from large bio-organic systems (as large as 9 kDa) is to combine a high magnetic field (19.6 T), a balanced probe circuit capable of generating strong radio frequency (RF) fields,³⁴ and the soft-pulse-added mixing (SPAM)³⁵ sequence.

Figure 1 shows the conventional one-dimensional (1D) ^{39}K MAS and corresponding two-dimensional (2D) high-resolution MQMAS NMR spectra of three organic solids: potassium picrate (KPic), $\text{K}_2(\alpha\text{-D-glucose 1-phosphate}) \cdot 2\text{H}_2\text{O}$ (KGP), and a lipophilic G-quadruplex structure (denoted as G_4 in this study) formed by self-assembly of $5'$ -*tert*-butyldimethylsilyl-2', 3'-*O*-isopropylidene guanosine (TBS-G) in the presence of KPic. Details of the sample preparations are given in the Supporting Information (SI). The 1D ^{39}K MAS spectrum of KPic exhibits a typical line shape arising from the second-order quadrupole interaction, suggesting the presence of a single K site in crystalline KPic. This observation is consistent with the crystal structure of KPic, in which there is only one K^+ ion in the asymmetric unit.³⁹ As shown in Figure 1a, the 2D ^{39}K MQMAS spectrum of KPic displays a sharp isotropic peak along the isotropic dimension (F_{iso}) with a full width at half height (fwhh) value of <1 ppm. For KGP, two K^+ signals are clearly observed (Figure 1b), in agreement with the crystal structure of KGP.⁴⁰ Remarkably, for G_4 , although the 1D ^{39}K NMR spectrum shows a featureless peak, the corresponding 2D MQMAS spectrum reveals the presence of four resolved ^{39}K signals (Figure 1c). While the spectral assignments for KPic and KGP are straightforward, the four ^{39}K signals observed for G_4 cannot be readily assigned. This lipophilic G-quadruplex structure, which is formed in the presence of KPic as illustrated in Scheme 1, is expected to have a structure similar to that formed by TBS-G self-assembly in the presence of mixed Cs and K picrates.⁴¹ To establish the ^{39}K NMR spectral assignment for G_4 unambiguously, we decided to determine the crystal structure of this lipophilic G-quadruplex

Received: June 7, 2011

Published: August 08, 2011

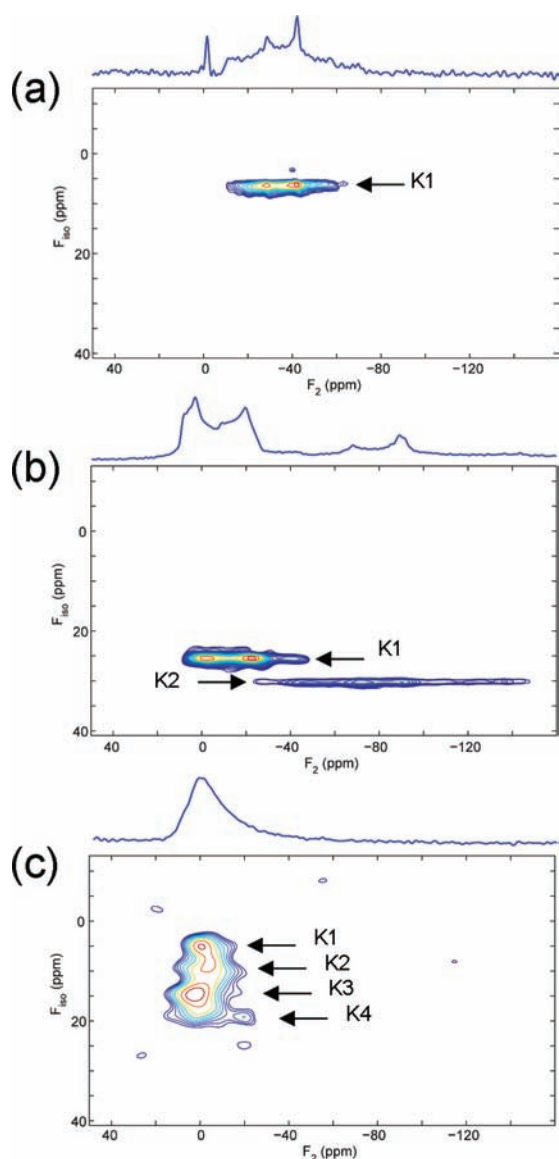


Figure 1. Experimental 1D MAS and 2D MQMAS ^{39}K NMR spectra of (a) KPic, (b) KGP, and (c) G_4 . Solid-state NMR experiments at 19.6 T were performed at the NMFML with a Bruker Avance console operating at 38.88 MHz for ^{39}K nuclei. A home-built 4 mm MAS probe using a balanced probe circuit was used. All ^{39}K chemical shifts were referenced to $\text{K}^+(\text{aq})$ at 0 ppm by setting the ^{39}K NMR signal from a solid KBr sample at 55 ppm. The sample spinning frequency was 8 kHz in all experiments. The pure absorptive 2D spectra were obtained by combining SPAM³⁵ with the shifted-echo method.^{36,37} The t_1 increment in the MQMAS experiment was synchronized with the sample spinning. The 3Q excitation and 3Q-to-1Q conversion pulses were 7.0 and 2.5 μs , respectively. The selective $\pi/2$ and π pulses were 6.0 and 10.0 μs , respectively. Other experimental details in the MQMAS experiments were as follows: KPic, 9600 transients for each t_1 , 26 t_1 increments, 1 s recycle delay; KGP, 9600 transients for each t_1 , 48 t_1 increments, 0.1 s recycle delay; G_4 , 48 000 transients for each t_1 , 40 t_1 increments, 0.1 s recycle delay. The very sharp signal at 0 ppm in (a) is due to the presence of a trace amount “liquidlike” micro domains in the solid sample of KPic. Along F_{iso} , 1 ppm = $34/9 \times \nu_0$, which is ca. 150 Hz for ^{39}K at 19.6 T. Here the factor $34/9$ stems from the “normalized” ppm scale as described by Amoureux et al.³⁸

(for crystallographic details, see the SI). As shown in Figure 2, this G-quadruplex structure consists of four G-quartets that are stacked on top of one another to form a central ion channel. The

Scheme 1

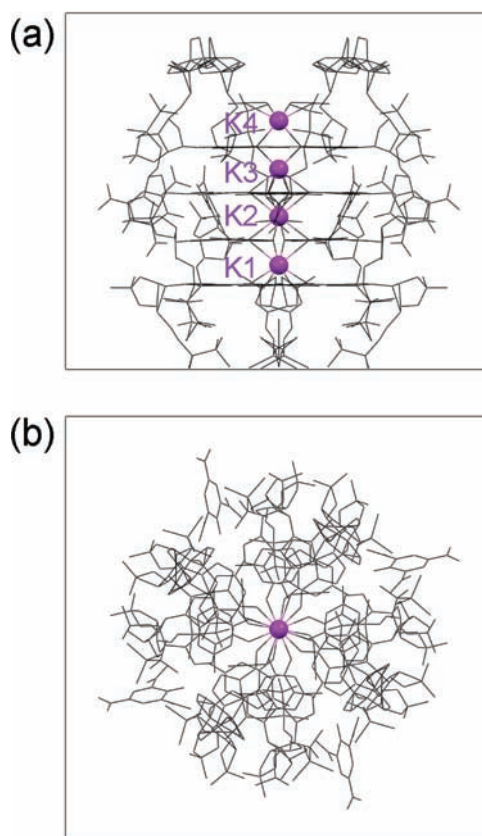
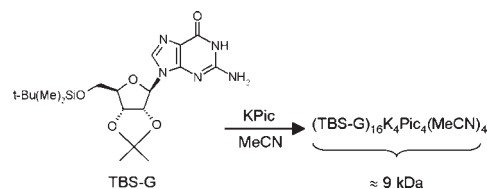


Figure 2. (a) Side view (along the crystallographic a axis) and (b) top view (along the crystallographic c axis) of a partial crystal structure of G_4 . The box marks the tetragonal unit cell.

G-quadruplex channel is fully occupied by three collinear K^+ ions, and one capping K^+ ion resides just outside one end of the channel. Each of the three K^+ ions in the channel is coordinated to eight carbonyl oxygen atoms from two adjacent G-quartet planes, with K–O distances ranging between 2.72 and 2.87 Å. The coordination environment around the capping K^+ ion is quite interesting. This K^+ ion is coordinated to four oxygen atoms from the end G-quartet (K–O distances: 2.93 Å) and four nitrogen atoms from the acetonitrile (solvent) molecules (K–N distances: 2.96 Å). This crystal structure provides an explanation of why a total of four ^{39}K signals are observed in the MQMAS spectrum of G_4 . However, as these four K^+ ions have similar chemical environments, it is still not obvious how to assign the four ^{39}K NMR signals to the four K^+ sites seen in the crystal structure.

As a further aid for the spectral assignment, we performed density functional theory (DFT) calculations of ^{39}K NMR parameters using a molecular cluster model based on the crystal structure of G_4 .

Table 1. Experimental and Computed ^{39}K isotropic Chemical Shifts (δ_{iso}), Quadrupolar Coupling Constants (C_Q), and Asymmetry Parameters (η_Q) For the Three Bio-organic Solids^a

system	site	^{39}K NMR Experiment			DFT Computation		
		δ_{iso} (ppm)	$ C_Q $ (MHz)	η_Q	δ_{iso} (ppm)	$ C_Q $ (MHz)	η_Q
KPic	K1	-7 ± 2	1.20 ± 0.02	0.60 ± 0.05	-10	1.32	0.55
KGP	K1	11 ± 2	1.17 ± 0.02	0.20 ± 0.05	18	1.51	0.36
	K2	-9 ± 2	1.85 ± 0.02	0.75 ± 0.05	-8	1.78	0.99
G_4	K1	3 ± 2	0.4 ± 0.1	0 ± 0.1	0	0.06	0.00
	K2	4 ± 2	0.8 ± 0.1	0 ± 0.1	0	0.70	0.00
	K3	12 ± 2	0.5 ± 0.1	0 ± 0.1	11	0.06	0.00
	K4	9 ± 2	1.0 ± 0.1	0.2 ± 0.1	-10	0.73	0.00

^a Experimental parameters were obtained from a combined analysis of 1D and 2D NMR spectra. DFT computational details are given in the SI.

To examine the computational consistency, we also performed similar calculations for KPic and KGP. Table 1 gives a summary of the experimental and computed ^{39}K NMR parameters for the three compounds. As shown in Table 1, the computed ^{39}K chemical shifts and quadrupole coupling constants are in reasonable agreement with the experimental results, except for the computed chemical shift for the capping K^+ ion (K4) in G_4 . As this capping K^+ ion is coordinated to four acetonitrile (solvent) molecules, the dynamic process of the solvent molecules may be the source of this discrepancy. Nonetheless, the computed ^{39}K NMR parameters allowed us to obtain the tentative spectral assignments as shown in Table 1. The observed ^{39}K NMR parameters for K1, K2, and K3 in G_4 are consistent with the spectral signature established for channel K^+ ions by both solution and solid-state NMR studies.^{17,42,43} We further note that the high resolution achieved in the ^{39}K MQMAS spectrum of G_4 is comparable to that observed in the ^{23}Na MQMAS spectra of analogous G-quadruplex structures,^{44,45} even though ^{39}K NMR spectroscopy is at least 200 times less sensitive than ^{23}Na NMR spectroscopy.

To provide a better understanding of the factors that determine the ultimate resolution limit in ^{39}K MQMAS NMR spectroscopy, we measured the ^{39}K transverse relaxation times (T_2) for the central transition (CT) signals in these compounds using a rotor-synchronized spin-echo sequence: KPic, 2.0 ± 0.5 ms; KGP, 16.0 ± 0.5 ms; G_4 , 4.0 ± 0.5 ms for all four K^+ sites. If we assume that the 3Q coherence ($m = +3/2 \leftrightarrow m = -3/2$) has a T_2 value similar to that for the CT in each system (it can be shown that in isotropic liquids, the nuclear quadrupole relaxation process has $T_2^{3Q} = T_2^{\text{CT}}$ for spin- $3/2$ nuclei),⁴⁶ the intrinsic fwhh values in the F_{iso} dimension of the ^{39}K MQMAS spectra would be ≤ 1.0 ppm for these compounds. As shown in Figure 1, the observed fwhh values are generally on the order of 0.8–2 ppm, approaching the estimated intrinsic values. Although our ^{39}K MQMAS experiments were performed without ^1H decoupling because of the limitation of the probe, ^1H – ^{39}K heteronuclear dipolar interactions are generally small in organic solids because of the low- γ nature of ^{39}K . For example, the largest ^1H – ^{39}K dipolar coupling constant in the systems studied here is 170 Hz for a ^1H – ^{39}K separation of 3.2 Å. Nonetheless, the observed nearly sub-ppm resolution is an important advancement in solid-state ^{39}K NMR spectroscopy that makes further chemical applications possible.

Now we turn our attention to a discussion of the sensitivity improvement achieved in this study, which is the key to the success of the reported ^{39}K MQMAS experiments. At the ^{39}K Larmor frequency, most commercial MAS probes (for 4 mm

rotors) typically can deliver a $\gamma B_1/2\pi$ field in the 20–30 kHz range. With the balanced probe circuit on our home-built MAS probe, the $\gamma B_1/2\pi$ field can reach ca. 70 kHz at $\nu_0 = 38.88$ MHz and is limited only by the maximum power output from a 1 kW amplifier. The basic idea of the balanced circuit is to split the tuning capacitor to two sides of the coil, which places the center of the coil at virtual ground. This arrangement reduces the peak voltage by a factor of 2 over an unbalanced circuit, thus enhancing the RF power handling capability to generate strong RF fields. As the balanced circuit has a narrow tuning range, it is not employed in commercial broadband MAS probes. However, as we have demonstrated in this study, the increased $\gamma B_1/2\pi$ field drastically enhances the sensitivity of the ^{39}K MQMAS experiment. A rather conservative estimate is that the combination of a balanced probe circuit and SPAM has boosted the sensitivity of the ^{39}K MQMAS experiment by a factor of 6–8, corresponding to an experimental time savings of a factor of 36–64. A more detailed examination of the benefits of using a balanced probe circuit in MQMAS experiments on low- γ nuclei was recently reported.³⁴

In summary, we have presented the first set of high-resolution ^{39}K MQMAS NMR spectra for bio-organic solids. Using a combination of high magnetic field (19.6 T), strong $\gamma B_1/2\pi$ fields, and the SPAM sequence, we were able to detect multiple distinct K^+ ions in a 9 kDa molecular system. This work also represents the first time that a biophysical technique other than X-ray crystallography has been shown to be capable of detecting different K^+ ions residing inside a G-quadruplex channel. The general approach demonstrated here should be applicable for probing K^+ ions in other biomolecular systems.

■ ASSOCIATED CONTENT

S Supporting Information. Details of sample preparation; molecular cluster models used in quantum-chemical computations; computational details; and tables of crystallographic data, atomic coordinates, thermal parameters, and selected bond lengths and angles. This material is available free of charge via the Internet at <http://pubs.acs.org>.

■ AUTHOR INFORMATION

Corresponding Author

gang.wu@chem.queensu.ca

Present Addresses

^{||} Department of Chemistry, University of California, One Shields Ave., Davis, CA 95616–5298.

ACKNOWLEDGMENT

G.W. thanks NSERC of Canada for financial support. All quantum-chemical calculations were performed at the High Performance Computing Virtual Laboratory (HPCVL) at Queen's University. I.C.M.K. thanks NSERC for a Canada Graduate Scholarship.

REFERENCES

- (1) Frausto da Silva, J. J. R.; Williams, R. J. P. *The Biological Chemistry of the Elements*; Oxford University Press: Oxford, U.K., 1991.
- (2) Lippard, S. J.; Berg, J. M. *Principles of Bioinorganic Chemistry*; University Science Books: Mill Valley, CA, 1994.
- (3) Page, M. J.; Di Cera, E. *Physiol. Rev.* **2006**, *86*, 1049.
- (4) Smith, M. E.; Van Eck, E. R. H. *Prog. Nucl. Magn. Reson. Spectrosc.* **1999**, *34*, 159.
- (5) Larsen, F. H.; Skibsted, J.; Jakobsen, H. J.; Nielsen, N. C. *J. Am. Chem. Soc.* **2000**, *122*, 7080.
- (6) Smith, M. E. *Annu. Rep. NMR Spectrosc.* **2001**, *43*, 121.
- (7) Toney, M. D.; Hohenester, E.; Cowan, S. W.; Jansonius, J. N. *Science* **1993**, *261*, 756.
- (8) Musayev, F. N.; Di Salvo, M. L.; Ko, T. P.; Gandhi, A. K.; Goswami, A.; Schirch, V.; Safo, M. K. *Protein Sci.* **2007**, *16*, 2184.
- (9) Larsen, T. M.; Benning, M. M.; Rayment, L.; Reed, G. H. *Biochemistry* **1998**, *37*, 6247.
- (10) Doyle, D. A.; Cabral, J. M.; Pfuetzner, R. A.; Kuo, A. L.; Gulbis, J. M.; Cohen, S. L.; Chait, B. T.; MacKinnon, R. *Science* **1998**, *280*, 69.
- (11) Morais-Cabral, J.; Zhou, Y.; MacKinnon, R. *Nature* **2001**, *414*, 37.
- (12) Zhou, Y. F.; Morais-Cabral, J. H.; Kaufman, A.; MacKinnon, R. *Nature* **2002**, *414*, 43.
- (13) Parkinson, G. N.; Lee, M. P. H.; Neidle, S. *Nature* **2002**, *417*, 876.
- (14) Haider, S.; Parkinson, G. N.; Neidle, S. *J. Mol. Biol.* **2002**, *320*, 189.
- (15) Adams, P. L.; Stanhley, M. R.; Kosek, A. B.; Wang, J.; Strobel, S. A. *Nature* **2004**, *430*, 45.
- (16) Stebbins, J. F.; Du, L.-S.; Kroeker, S.; Neuhoff, P.; Rice, D.; Frye, J.; Jakobsen, H. J. *Solid State Nucl. Magn. Reson.* **2002**, *21*, 105.
- (17) Wu, G.; Wong, A.; Gan, Z.; Davis, J. T. *J. Am. Chem. Soc.* **2003**, *125*, 7182.
- (18) Wong, A.; Whitehead, R. D.; Gan, Z.; Wu, G. *J. Phys. Chem. A* **2004**, *108*, 10551.
- (19) Widdifield, C. M.; Schurko, R. W. *J. Phys. Chem. A* **2005**, *109*, 6865.
- (20) Duxson, P.; Provis, J. L.; Lukey, G. C.; van Deventer, J. S. J.; Separovic, F.; Gan, Z. H. *Ind. Eng. Chem. Res.* **2006**, *45*, 9208.
- (21) Moudrakovski, I. L.; Ripmeester, J. A. *J. Phys. Chem. B* **2007**, *111*, 491.
- (22) Lee, P. K.; Chapman, R. P.; Zhang, L.; Hu, J.; Barbour, L. J.; Elliott, E. K.; Gokel, G. W.; Bryce, D. L. *J. Phys. Chem. A* **2007**, *111*, 12859.
- (23) Michaelis, V. K.; Aguiar, P. M.; Kroeker, S. *J. Non-Cryst. Solids* **2007**, *353*, 2582.
- (24) Wu, G.; Tersikh, V. *J. Phys. Chem. A* **2008**, *112*, 10359.
- (25) Samoson, A.; Lippmaa, E.; Pines, A. *Mol. Phys.* **1988**, *65*, 1013.
- (26) Chmelka, B. F.; Mueller, K. T.; Pines, A.; Stebbins, J.; Wu, Y.; Zwanziger, J. W. *Nature* **1989**, *339*, 42.
- (27) Wu, Y.; Sun, B. Q.; Pines, A.; Samoson, A.; Lippmaa, E. *J. Magn. Reson.* **1990**, *89*, 297.
- (28) Llor, A.; Virlet, J. *Chem. Phys. Lett.* **1988**, *152*, 248.
- (29) Mueller, K. T.; Sun, B. Q.; Chingas, G. C.; Zwanziger, J. W.; Terao, T.; Pines, A. *J. Magn. Reson.* **1990**, *86*, 470.
- (30) Frydman, L.; Harwood, J. S. *J. Am. Chem. Soc.* **1995**, *117*, 5367.
- (31) Medek, A.; Harwood, J. S.; Frydman, L. *J. Am. Chem. Soc.* **1995**, *117*, 12779.
- (32) Gan, Z. *J. Am. Chem. Soc.* **2000**, *122*, 3242.
- (33) Dowell, N. G.; Ashbrook, S. E.; Wimperis, S. *J. Phys. Chem. B* **2004**, *108*, 13292.
- (34) Gan, Z.; Gor'kov, P. L.; Brey, W. W.; Sideris, P. J.; Grey, C. P. *J. Magn. Reson.* **2009**, *200*, 2.
- (35) Gan, Z.; Kwak, H. T. *J. Magn. Reson.* **2004**, *168*, 346. There are errors in this paper with regard to the phase of the SPAM soft pulse. A SPAM soft pulse with reverse phase relative to the mixing pulse should enhance the $|\Delta p| = 2$ coherence transfer pathway, and the one with the same phase should enhance the $|\Delta p| = 4$ coherence transfer pathway.
- (36) Grandinetti, P. J.; Baltisberger, J. H.; Llor, A.; Lee, Y. K.; Werner, U.; Eastman, M. A.; Pines, A. *J. Magn. Reson., Ser. A* **1993**, *103*, 72.
- (37) Massiot, D.; Touzo, B.; Trumeau, D.; Coutures, J. P.; Virlet, J.; Florian, P.; Grandinetti, P. J. *Solid State Nucl. Magn. Reson.* **1996**, *6*, 73.
- (38) Amoureux, J. P.; Huguenard, C.; Engelke, F.; Taulelle, F. *Chem. Phys. Lett.* **2002**, *356*, 497.
- (39) Harrowfield, J. M.; Skelton, B. W.; White, A. H. *Aust. J. Chem.* **1995**, *48*, 1311.
- (40) Sugawara, Y.; Iwasaki, H. *Acta Crystallogr., Sect. C* **1984**, *40*, 389.
- (41) Forman, S. L.; Fettingter, J. C.; Pieraccini, S.; Gottarelli, G.; Davis, J. T. *J. Am. Chem. Soc.* **2000**, *122*, 4060.
- (42) Wong, A.; Ida, R.; Wu, G. *Biochem. Biophys. Res. Commun.* **2005**, *337*, 363.
- (43) Ida, R.; Kwan, I. C. M.; Wu, G. *Chem. Commun.* **2007**, 795.
- (44) Wong, A.; Fettingter, J. C.; Forman, S. L.; Davis, J. T.; Wu, G. *J. Am. Chem. Soc.* **2002**, *124*, 742.
- (45) Wu, G.; Wong, A. *Biochem. Biophys. Res. Commun.* **2004**, *323*, 1139.
- (46) Jaccard, G.; Wimperis, S.; Bodenhausen, G. *J. Chem. Phys.* **1986**, *85*, 6282.